RESEARCH ARTICLE VOLCANICA

Thick crust, hydrous magmas, and the paradox of voluminous cold magmatism

Cin-Ty A. Lee*, Boda Liu
Department of Earth, Environmental and Planetary Sciences, Rice University, Houston, TX, USA

Abstract

Ocean-continent subduction zones are important for making continental crust. Here, long chains of magmatic mountain belts, known as continental arcs, and the key characteristics of continental crust – thick crust and andesitic to dacitic compositions – are made. Andesitic to dacitic magmas are thought to derive from basaltic parents generated from the mantle, but only after significant cooling and crystallization of a basaltic magma or by low degree re-melting of basaltic crust. How massive batholiths are generated from such refined and "cold" magmas is unclear. Using a case study of a Cretaceous batholith in southern California (USA), we show that large intermediate (57–68 wt. % SiO_2) plutons are favored when the arc crust attains thicknesses of 30–60 km whereas mafic, gabbroic plutons (<55 wt. % SiO_2) are small and favored during the early stages of an arc when the crust is thin (<30 km). We explore simple thermal models of arc crust to show that large, long-lived and relatively cold partially molten zones, sustained by recharge of hydrous basaltic magmas, are favored in the lower crust when arc crust is thick. This is due to the reduced efficiency of heat loss to the surface with increasing crustal thickness . In contrast, thin crust and drier magmas favor hotter and thinner partially molten zones. Our models and observations provide an explanation for the seemingly paradoxical observation that the most voluminous magmas in continental arc settings are relatively cold (800–1000 °C). If crustal thickness is important for making andesitic and dacitic magmas, their origins must be linked to the interplay between magmatic differentiation, the availability of water, and the collective processes that control crustal thickness in magmatic arcs: magmatism, tectonism, and erosion.

Keywords: `Pluton; Cordillera; Continental arc; Andesite; Partially molten zone`

1 Introduction

The origins of intermediate magmas, such as andesites and dacites and their intrusive equivalents (granodiorites and tonalites), have long been debated because of their importance in arc systems. Many hypotheses have been proposed. A simple hypothesis for the origin of intermediate magmas is that they form by progressive crystal fractionation of a hydrous parental basalt [Lee 2014; Blatter et al. 2017]. However, other models include mixing between mafic and felsic magmas [Reubi and Blundy 2009; Blatter et al. 2017], water-saturated melting of the mantle [Kelemen et al. 2007; Grove et al. 2012], re-melting of the lower crust [Draut et al. 2002; Collins et al. 2016; 2020], re-melting of subducted oceanic crust [Rapp et al. 2003; Martin et al. 2005], melting of hybridized mantle [Lara and Dasgupta 2020], and enhanced melt productivity at the intermediate temperatures that favor andesitic melts [Reubi and Blundy 2009]. Whatever their origin, andesites, dacites and their intrusive equivalents have long been thought to be most prevalent in thick continental arcs like the modern Andes, an observation confirmed by the fact that the silica contents of arc volcanics correlate with elevation and crustal thickness [Farner and Lee 2017]. As we will show here, these relatively cold, intermediate magmas also form the largest plutons. This poses a dilemma. Except for those derived directly from the mantle, intermediate magmas are likely derivative liquids, and thus should be colder and of lower volumes than their mafic counterparts. Even during water-saturated melting of the mantle, the total amounts of intermediate magmas generated directly from the mantle should be small compared to that of basalts. Why then do intermediate magmas generate the largest plutons and why are they most abundant in volcanic arcs, particularly those characterized by thick crust?

2 Methods and Results

To gain insight into the origin of andesitic and dacitic magmas, we synthesized geochemical, geochronologic and geochemical data for the Cretaceous northern Peninsular Ranges Batholith (PRB) in southern California, USA (Figure 1). This batholith was formed by eastward subduction of the Farallon oceanic plate beneath the margin of western North America [Lee et al. 2007; Morton et al. 2014b]. The prebatholithic structure consists of a Jurassic oceanic arc that was accreted onto the margin of the North American continent. Continental arc magmatism initiated ~130 Ma, first through the accreted terranes and gradually migrating eastward across the suture and into the ancient continental mar-

*Corresponding author: ctlee@rice.edu

gin, terminating ~80 Ma.

Average pluton compositions were calculated from a previously published geochemical dataset [Lee et al. 2007; Morton et al. 2014a; b]. This dataset is unique in that sampling strategy was designed to minimize small, meter–scale heterogeneities (meter scale), a persistent problem with many plutonic rocks, which often contain mafic schlieren. The database utilizes rock samples collected from each of the four corners of a 122 × 122 meter square [Baird et al. 1979]. Two samples from each corner were collected, making a total of 8 samples per locality, all of which were mixed together to generate a homogeneous mixture that is representative of the pluton on the 122 × 122 m length scale (equivalent to 400 × 400 feet square; the Imperial system was used in the original study). These 122 × 122 meter sampling schemes were reproduced throughout the Peninsular Ranges Batholith on uniformly spaced grids in a given pluton (1–4 km spacing, depending on pluton). To obtain the average composition of a pluton, we first adopted the mapped boundaries of the plutons as defined by geochronologic, compositional, and textural similarities [Morton et al. 2006; Morton et al. 2014b]; significantly tilted plutons or plutons with unmapped boundaries were not included in this study. We then averaged over each sampling grid point within a pluton to obtain the average composition of each pluton. Data as well as averages and standard deviations are shown in Supplemental Tables 1 and 2.

Overall, the compositions of individual plutons are highly variable, ranging from gabbros (basaltic and basaltic andesitic) with ~50 wt. % SiO_2 to granites (rhyolitic) with >70 wt. % SiO_2 [Lee et al. 2007; Morton et al. 2014b]. However, on average, the entire batholith is andesitic to dacitic in composition, and hence of intermediate composition. In detail, the older western zones are slightly more mafic than the younger eastern zones (Figures 1 and 2 A, B), with gabbro restricted to the western zone. Element ratios, such as Gd/Yb, which are sensitive to garnet fractionation and hence provide a constraint on average pressures of differentiation, indicate that crustal thickness was about 30–40 km in the western zones and 60–80 km in the eastern zones (Figure 2C) [Lee et al. 2007; Morton et al. 2014b; Farner and Lee 2017].

Two important observations come out of our data synthesis. The first comes from comparing the average compositions of the plutons with their mapped areas (Figure 1). Gabbroic plutons tend to be small, never exceeding 20–30 km^2 (Figures 1 and 2D). In contrast, felsic plutons range from small (50 km^2) to large (500 km^2), but maximum pluton area increases with increasing SiO_2, reaching a maximum at andesitic to dacitic compositions (60–70 wt. % SiO_2) and decreasing again for silica contents >70 wt. % (Figure 2D). Although biases in relative pluton size are introduced by not considering the vertical dimension, the 10-fold difference in maximum areas of intermediate and mafic plutons exceed possible uncertainties in the vertical dimension. Zirconium saturation temperatures indicate that the intermediate magmas were relatively cold (700–850 °C) compared to their mafic parents (900–1200 °C) [Lee 2014]. Thus, a key observation is that the largest plutons represent relatively cold, intermediate magmas and are predominantly found in the eastern zones where the crust was thickest.

The second key observation is that plutons within their respective western and eastern zones fall along a shared covariation of the major and minor elements [Lee et al. 2007; Morton et al. 2014b]. For example, all plutons fall along a trend in which MgO decreases monotonically with increasing SiO_2 and P_2O_5 peaks at intermediate SiO_2 contents. The coherence of the plutons to the same differentiation trend suggests a common liquid line of descent. However, not only are these plutons separated by many tens of km, they are also not coeval as crystallization ages differ by 50 My [Kistler et al. 2003], far longer than the assembly times of an individual pluton (100 ky to 1 My) [Barboni et al. 2015] These compositional similarities indicate a common formation process, but the plutons are not directly derived from one another in space and time. More likely, these plutons are tapped at different times from a long-lived lower crustal partially molten zone (PMZ) [Hildreth and Moorbath 1988; Annen et al. 2005; Bachmann and Bergantz 2008]. The nonlinear trend in P_2O_5 versus SiO_2 suggests that differentiation is dominated by crystal fractionation with crustal assimilation or mixing between mafic and felsic magmas of lesser, but not negligible, importance [Lee 2014].

3 Insights

3.1 Thermal models

To better understand why large, cold plutons preferentially form in thick crust and why all plutons, regardless of age and location, seem to share a similar liquid line of descent, we modeled the thermal state of a lower crustal PMZ. We envision the PMZ to be a magmatic mush layer (crystals + melt) of thickness H undergoing simultaneous crystallization and recharge of a hotter magma (Figure 3). The base of the PMZ coincides with the base of the crust. The top of the layer is defined by the transition from a partially molten state to the melt-free crustal lid as defined by the intersection between the geotherm and the rock's solidus (a water saturated system is assumed [Collins et al. 2016; 2020]. Heat is lost from the PMZ by cooling through the overlying crustal lid or by advective loss through upwards expulsion of interstitial liquids. As it cools, the PMZ crystallizes. Crystals may stay suspended within the mushy PMZ, but any crystals that segregate downwards are considered to exit the PMZ and return to the mantle (via foundering or delamination).

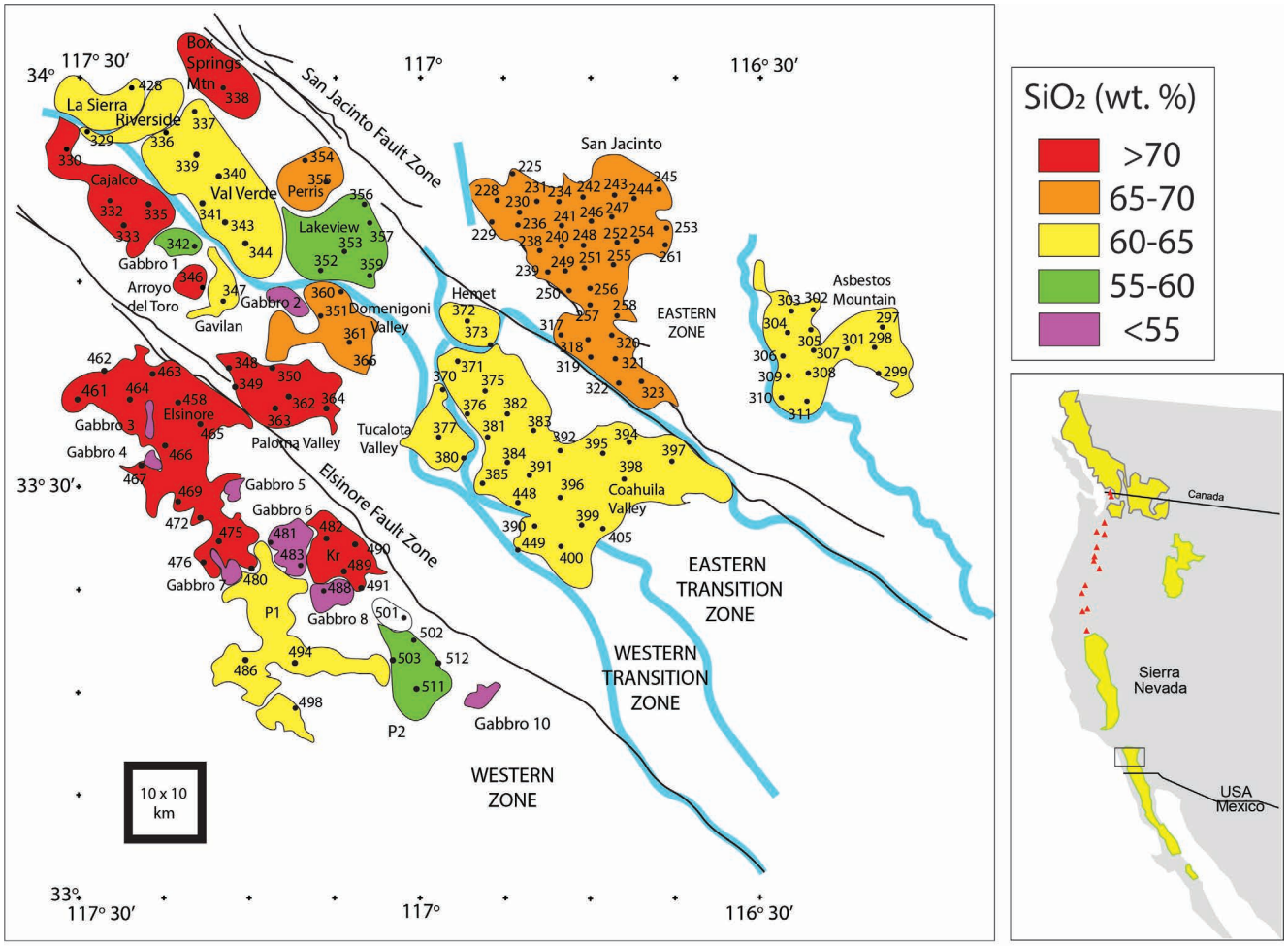

Figure 1: Geologic map of plutons in the northern Peninsular Ranges Batholith in southern California, USA. Plutons are color-coded according to average SiO_2 content (wt. %). Names of sampling locations and the host pluton are denoted. Thin black lines correspond to active faults associated with the San Andreas fault zone. Thick gray lines delineate boundaries between different zones of the batholith as determined from age, pluton texture, and pre-batholithic lithologies and structure. Eastern plutons average more silicic than western plutons. Inset on lower right shows location of the batholith in relation to Cretaceous batholiths (yellow) in western North America and active arc volcanoes in the Cascades. Note that only those plutons whose boundaries can be delineated are shown. Unmapped or undivided plutonic rocks are not shown. Sample locations, pluton boundaries, and geologic features compiled from Morton et al. [2006], Lee et al. [2007], and Morton et al. [2014a,b].

We approximate the lower crustal PMZ's temperature by an effective average temperature, regardless of whether it is convectively or conductively cooling because we assume that the overlying crustal lid is much thicker than the PMZ (as shown later, the PMZ does not exceed 20 % of the total crustal thickness), so that heat loss is controlled by the crustal lid overlying the PMZ. The energy balance for the PMZ is [Liu and Lee 2020]:

$$\frac{d}{dt}(\rho_{PMZ}c_{PMZ}T_{PMZ}H) \sim \rho_{mi}c_{mi}T_{in}J_{in} - \rho_{me}c_{me}T_{PMZ}J_e - \rho_x c_x T_{PMZ}J_x + \rho_m HL\frac{dF}{dT}\frac{dT_{PMZ}}{dt} - k\frac{T_{PMZ}}{Z} + q_0 \quad (1)$$

where ρ and c are the densities and heat capacities of the PMZ, incoming melt (mi), erupted residual melt (me), and solid crystal cumulates (x); T_{PMZ} is the temperature of the PMZ; T_{in} is the temperature of the incoming melt; J_{in} is the volume flux of incoming melt ($\mathrm{m\,yr^{-1}}$); J_e is the volume flux of residual liquid expelled or erupted from the mushy PMZ; J_x is the volume flux of crystals settling out of the PMZ; H is the thickness of the PMZ; L is latent heat; F represents how melt fraction varies with temperature; k is thermal conductivity; Z is the depth to the center of the PMZ; and q_o is the basal mantle heat flux ($\mathrm{W\,m^{-1}}$). The first term on the right represents heat advected in by magma recharge, the second is heat loss by melt evacuation, the third is heat loss by crystals exiting the system, the fourth is latent heat, the fifth is conductive heat loss to the surface, and the last is the conductive basal heat flow into the PMZ. The conductive heat loss term is the product of the temperature gradient multiplied by the

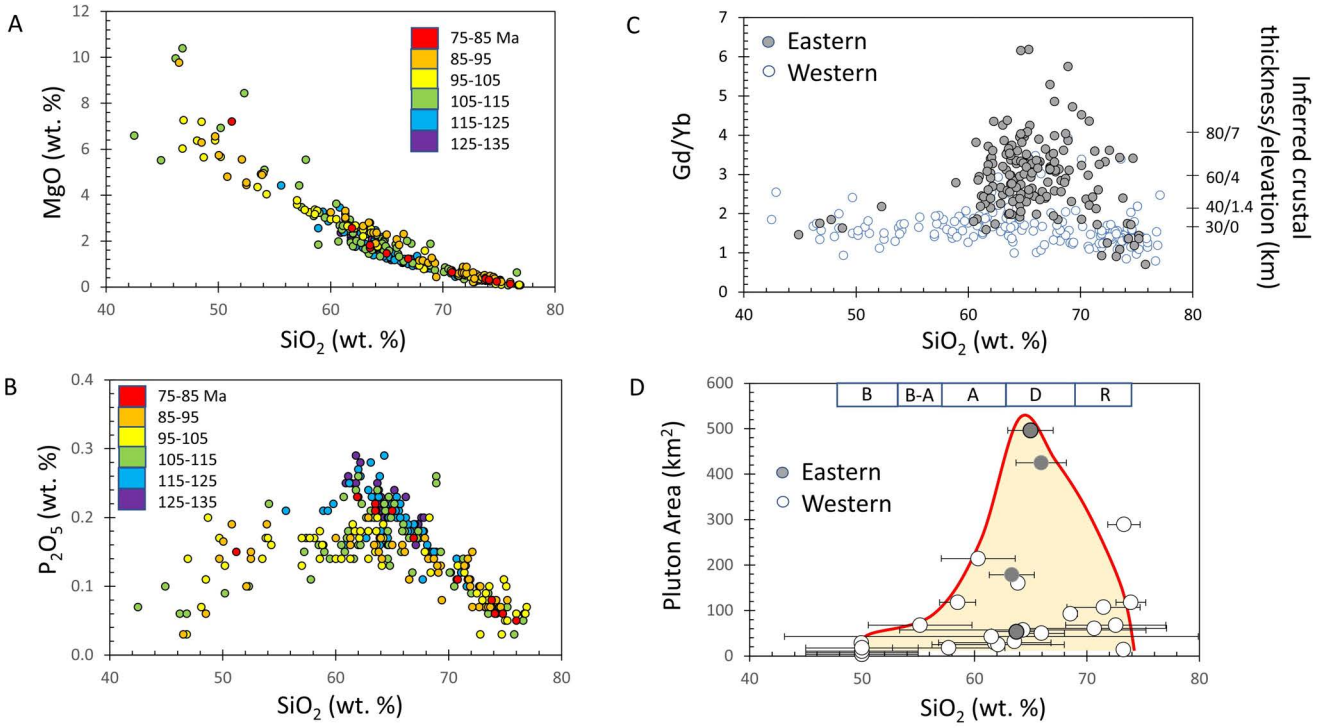

Figure 2: Compositional characteristics of the northern Peninsular Ranges Batholith. [A] MgO versus SiO_2 (wt. %) color-coded according to crystallization age. [B] P_2O_5 versus SiO_2 (wt. %) color-coded according to crystallization age. [C] Gd/Yb (ppm/ppm) versus SiO_2 (wt. %). Gray symbols represent Eastern and Eastern Transition Zone samples and open symbols represent Western and Western Transition Zone samples from Figure 1. Right hand axis corresponds to approximate crustal thickness and elevation inferred from global empirical relationships between Gd/Yb and elevation of arc volcanoes. The first number represents crustal thickness and the second represents elevation (km). Data are based on published literature [Lee et al. 2007; Morton et al. 2014b]. [D] Pluton area (km^2) versus average SiO_2 content of the pluton (see Table 1). Horizontal error bars represent 1 standard deviation for SiO_2. It is impossible to estimate internal errors on estimates of pluton area; a more relevant issue is the accuracy and representativeness of pluton area as pluton volume (see text). Gray symbols represent Eastern and Eastern Transition Zone plutons and white symbols represent Western and Western Transition Zone plutons. Red line represents a qualitative bounding line defining the maximum pluton sizes. Symbols in top horizontal bar correspond to the fields for rhyolite (R), dacite (D), andesite (A), basaltic-andesite (B-A), and basalt (B).

thermal conductivity of the rock, the former approximated by dividing the temperature T_{PMZ} of the PMZ by the depth Z of the PMZ (surface temperature is taken as 0 °C). To account for hydrothermal cooling, a high effective thermal conductivity can be adopted, but we have chosen not to do this here because we have no constraints on hydrothermal processes. In the above formulation, crustal radioactivity is ignored as it is smaller than the magmatic advection of heat.

Equation 1 is a quantitative treatment of the MASH zone concept (Melting, Accumulation, Storage, and Homogenization) [Hildreth and Moorbath 1988], which qualitatively describes a lower crustal zone undergoing melting, assimilation, storage, and homogenization. In the MASH model, hot magmas can assimilate and remelt pre-existing crust, which is implicitly accounted for in Equation 1 through the latent heat term. However, the MASH concept requires, but does not explicitly include magmatic recharge, which is necessary for re-melting and assimilation. Our approach follows the more general framework of a magmatic system undergoing simultaneous recharge, eruption/evacuation and fractional crystallization [Bohrson and Spera 2007; Bohrson et al. 2014; Lee 2014]. In this model, remelting of basalts, whether by hydrous flux melting or heating [Collins et al. 2016; 2020], is implicitly included as long as it is assumed that all of these components (magmas and previously crystallized rocks) are included within the PMZ.

We can consider the case in which the temperature of the PMZ and its thickness are at steady state, T^{SS}_{PMZ}. Because steady state requires that $J_{in} = J_e + J_x$, the steady state temperature of the PMZ is given by

$$T^{ss}_{PMZ} \sim \frac{J_{in}T_{in} + q_o/\rho c}{J_{in} + \kappa/Z} = \frac{T_{in} + q_o/\rho c J_{in}}{1 + \kappa/Z J_{in}} \quad (2)$$

where κ is thermal diffusivity ($k/(\rho c)$). For simplicity, the densities and heat capacities of melts, crystals and the mush (crystals + melt) making up the PMZ are assumed to be the same because the largest uncertainties

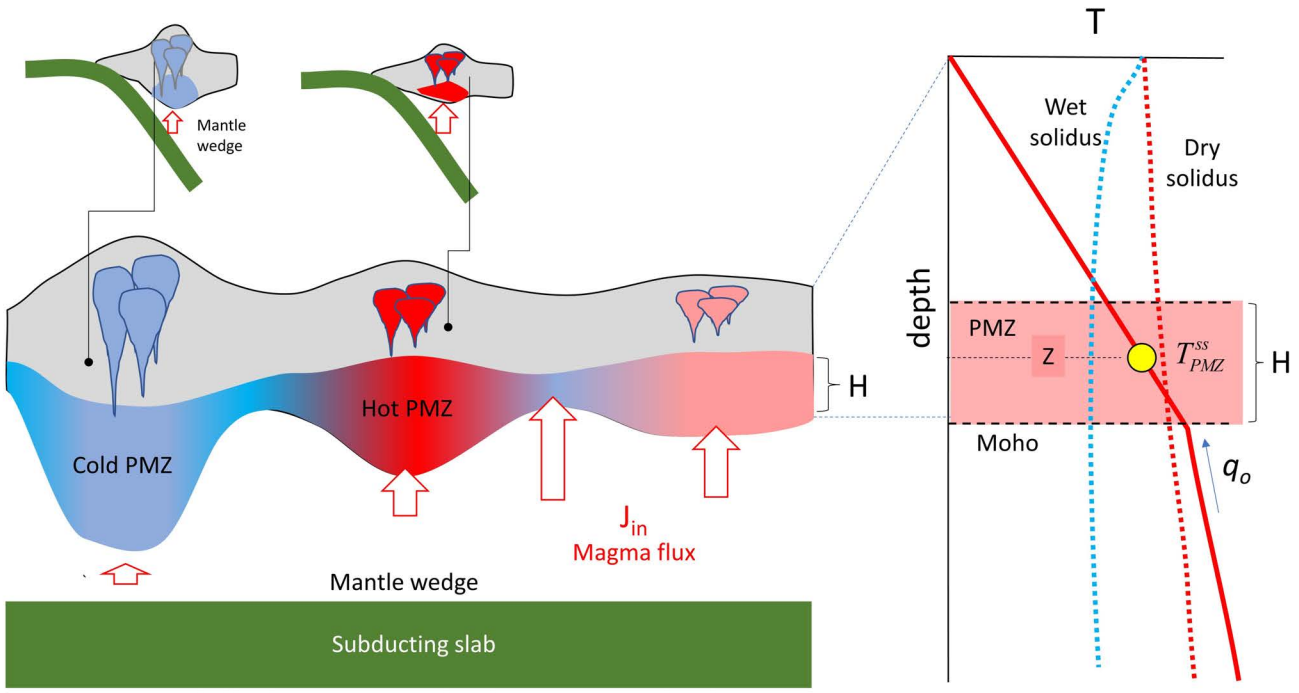

Figure 3: Conceptual cartoon of a lower crustal Partially Molten Zone (PMZ) in volcanic arcs. Base of the PMZ corresponds to the base of the arc crust. Top of the PMZ corresponds to the transition from a partially molten lower crust to a cold, melt-free crust. This transition is controlled by the intersection of the geotherm (red line in graph) with the water-saturated solidus (blue line). Beneath the arc crust lies the convecting asthenospheric mantle wedge (and a thin lithospheric mantle). This mantle wedge is underlain by the subducting slab (oceanic lithosphere), which ultimately drives upwelling within the mantle wedge. Such upwelling drives decompression melting of the mantle, leading to a magmatic flux J_{in} into the PMZ. As crustal thickness increases (Z), J_{in} decreases. The PMZ is characterized by a thickness H and a steady state temperature T^{SS}_{PMZ}. Temperature of the PMZ is controlled by conductive heat loss through the solid upper crust and heat gain from below via magmatic recharge J_{in} and a basal conductive heat flow q_o from the mantle.

are in other terms, such as J_{in}, and q_o. At steady state, it is important to note that the latent heat term cancels. It can be seen that T^{SS}_{PMZ} scales positively with recharge rate J_{in} and depth Z of the PMZ, the latter controlling efficiency of heat loss (Equation 2). For a given q_o, T^{SS}_{PMZ} scales with the dimensionless Recharge number, $R = ZJ_{in}/\kappa$, which represents the relative strength of recharge heat versus heat loss, akin to a Peclet number in diffusion-advection systems. When R is large, T^{SS}_{PMZ} approaches the temperature of the recharging magma if q_o is zero. When R is small and the heat loss is more efficient than recharge, T^{SS}_{PMZ} approaches the background temperature of the crust as sustained by basal heat flow q_o. Thus, recharge buffers the temperature of the PMZ. If recharge can be sustained by magmas originating from the mantle, a long-lived PMZ in the lower crust can persist at any magmatic temperature, depending on the characteristic Recharge number. Steady state mush temperatures can be increased with higher basal heat flow q_o or decreased with increased hydrothermal activity. Equation 2 can also be used to approximate steady state thickness of the PMZ, H,

$$H \sim 2(1 - T_s/T^{ss}_{PMZ})Z \tag{3}$$

where T_s is the temperature of the solidus. This estimate of steady state thickness assumes the temperature in the PMZ is linear with depth. This approximation is crude because we assume steady state and that the temperature profile is linear from the surface of the Earth to the base of the PMZ. We also assume in the energy balance of Equation 1 that the temperature of the PMZ can be treated with an effective average temperature T^{SS}_{PMZ}. While our model setup fails to describe all the detailed physics, its simplicity does allow us to see what the first order controls are. The PMZ thickness scales with its depth beneath the surface (and crustal thickness) and its steady state temperature T^{SS}_{PMZ}. Because T^{SS}_{PMZ} scales with J_{in}, H increases with increasing J_{in}.

If magma recharge is linked to decompression melting in the mantle wedge, then recharge rate should vary with lithospheric thickness, which limits the extent of decompression melting in the wedge as well as wedge temperature [England and Katz 2010; Karlstrom et al.

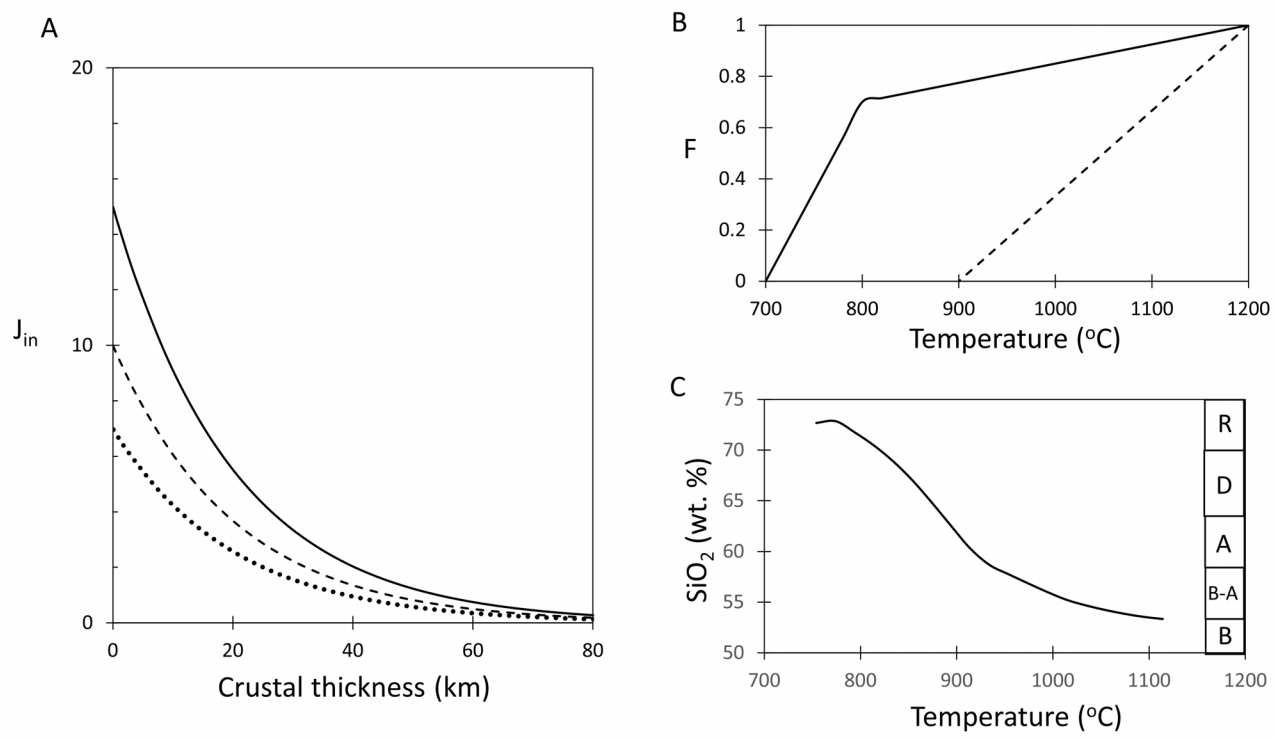

Figure 4: [A] Modeled magmatic flux J_{in} as a function of crustal thickness. J_{in} at zero crustal thickness corresponds to J_{in}^{o} , the hypothetical baseline magmatic flux from the mantle, which we equate with the baseline recharge flux. J_{in} decays exponentially with increasing crustal thickness because thick crust limits the extent of decompression melting in the mantle. [B] Idealized melt productivity curves for hydrous and anhydrous systems used in models. Given variability based on different starting compositions, we use simple parameterizations to capture first order behaviors. Under hydrous conditions, solidus is depressed and melt productivity curve is highly nonlinear. [C] SiO_2 of melt was not calculated in our models, but shown here for context is an approximate relationship of the SiO_2 content of residual melt versus temperature for a basaltic bulk composition with 4 wt. % H_2O at 0.3 GPa as determined from thermodynamic modeling [Lee and Bachmann 2014]. This curve is dependent on the conditions of crystallization as the exact nature of the curve depends on pressure, bulk composition and water content. Symbols on the right correspond to rhyolite (R), dacite (D), andesite (A), basaltic-andesite (B-A), and basalt (B).

2014; Turner et al. 2016]. In typical arcs, the lithospheric mantle is thin so the crust dominates the thickness of the lithosphere and recharge rate decreases with increasing crustal thickness. This relationship is parameterized by allowing J_{in} to decrease exponentially with crustal thickness (Figure 4A),

$$J_{in}(Z) = J_{in}^{o} exp(-Z/\delta) \quad (4)$$

Here, Z is an approximation of crustal thickness because the PMZ is located at the base of the crust and is significantly thinner than the total crustal thickness. J_{in}^{o} is a hypothetical baseline magmatic flux ($km^2\,Myr^{-1}$) when the crustal thickness is zero and can be approximated by considering the magmatic flux in a given arc and extrapolating to zero crustal thickness. The characteristic depth over which magmatic flux decays with crustal thickness is δ. Slab-derived fluids, which cause freezing point depression, changes J_{in}^{o}, but should not significantly change how magmatic flux decays with crustal thickness.

3.2 Limitations of the model

We emphasize that our model is simplistic in many of its assumptions, so we recognize that our model cannot be used to accurately describe geologic reality. The purpose of our simplified thermal modeling is only to capture zeroth order trends and behavior, not exact numbers. We expand on some of these limitations here.

Our treatment of the lower crustal PMZ as a reservoir with an effective temperature is essentially an idealized box model that does not account for where and how magmas are emplaced in the lower crust (e.g. diking, diapirism, etc.), how magmas and crystals separate, and the physics by which heat is transported within and out of the system by convective processes. Incorporating any of these processes would also require full incorporation of rheological laws for multiphase suspensions or a particle dynamics approach. All these processes are unrealistically lumped in our simplified box model, but their integrated effects can be qualitatively

explored by changing parameters in our model.

Another simplification of our analysis is the assumption of steady state in terms of heat and mass balance. Steady state is only valid if the response time of the PMZ to thermal and mass perturbations is shorter than the lifespan of an arc. Approximate mass response times can be estimated by dividing the steady state thickness of the PMZ by magma recharge rate. Except for thicknesses exceeding 80 km, when recharge rate is very low, estimated mass response times are less than 10 My, which is shorter than the lifespan of a continental arc (~50 My) [Ducea et al. 2015]. Thermal response time, however, is far more problematic for our model because a potential rate-limiting process is heat transfer through the overlying crustal lid, which is slow if it is controlled by conduction. The thermal response time of the overlying crustal lid scales as Z^2/κ, which for a thermal diffusivity of 10^{-6} $m^2 s^{-1}$ is ~30 My for a PMZ lying at depths of 30 km or ~120 My for PMZs lying at 60 km depth. Clearly, for PMZs in thick crust, it is unlikely that steady state in terms of heat balance is achieved within the lifetime of a magmatic arc segment. We note, however, that the thermal response of the crustal lid is complicated by the likelihood of hydrothermal convection, which increases effective thermal diffusivity (possibly by more than a factor of 2) and decreases thermal response time [Cao et al. 2019].

4 Controls on PMZ thickness and melt composition

We consider three different baseline recharge rates J_{in}^{o} from the mantle (7, 10, and 15 $km^3 km^{-2} My^{-1}$) with a characteristic exponential decay length scale of 20 km to ensure that J_{in} decays to zero by 80 km when the mantle wedge is too thin to support melting, causing magmatism to terminate [Karlstrom et al. 2014; Chin et al. 2015] (Figure 4A). We consider a representative baseline mantle flux of 10–15 $km^3 km^{-2} My^{-1}$ as representative, based on extrapolating the magmatic flux of continental arcs to a crustal thickness of zero (magmatic flux estimated from the pluton flux—1–2 $km^2 Myr^{-1}$—plus the production of mafic cumulates of >66 % [Lee 2014; Jiang and Lee 2017]). The temperature of the recharging magma is taken as 1200 °C, which we also use to define the liquidus temperature of the magma.

An important relationship is how melt fraction F varies with temperature. Here, we approximate this behavior with simple functions (Figure 4B, C). These functions are not meant to reproduce experimental data on natural systems exactly but rather to capture general behavior. Thus, for a completely anhydrous system, we adopt a linear T-F relationship with a solidus at 900 °C and a liquidus at 1200 °C. The solidus of 900 °C is similar to the liquidus of anhydrous rhyolites from the Yellowstone hotspot [Almeev et al. 2012]. For hydrous systems, the solidus is depressed by a couple hundred degrees, and the T-F relationship is strongly nonlinear due to eutectic-like crystallization/melting in which most of the melt productivity occurs close to the water-saturated solidus [Hartung et al. 2019]. We adopt 700 °C as the solidus of hydrous basaltic systems, but assume the liquidus temperature remains the same (this is reasonable if water is a conserved quantity). The nonlinearity of $F(T)$ is described as two linear segments between a water-saturated solidus of 700 °C and a 1200 °C liquidus; we consider the system 70 % molten at 800 °C for a hydrous system [Lee et al. 2015a].

For thermal modeling, we adopt a typical thermal diffusivity of 30 $km^2 Myr^{-1}$ (thermal conductivity k is assumed to be 2.5 $W m K^{-1}$). We adopt a basal mantle heat flow q_o of 15 $mW m^{-2}$, which we estimated by taking the lowest surface heat flow observed in continental arc systems [Till et al. 2019] and subtracting crustal radioactivity. As stated above, for the purposes of this paper, we did not consider heat advection by erosion or hydrothermal circulation in the upper crust.

In Figures 5 and 6A, we plot the results for hydrous systems. The average steady state temperature T_{PMZ}^{SS} of the lower crustal PMZ is plotted against crustal thickness, along with the corresponding values of melt fraction F, thickness H of the PMZ, and the total available volume of melt in the PMZ, which is the product of F and H. The temperature T_{PMZ}^{SS} of the PMZ increases initially with crustal thickness because the increase in Z dominates the Recharge number, thereby decreasing the efficiency of heat loss. Cold temperatures <750 °C are predicted for crustal thicknesses <25 km because of efficient heat loss, but as crustal thickness increases, heat loss becomes inefficient and temperature rises. Further increase in crustal thickness causes J_{in} and the Recharge number to decrease, which causes temperature to decrease again. Maximum temperatures T_{PMZ}^{SS} (>900 °C) exist at crustal thicknesses of ~30 km with temperatures declining to <800 °C as crustal thicknesses exceed ~60 km. The thickness of the lower crustal PMZ also increases with crustal thickness due to the inefficiency of heat loss as the crust thickens. However, the thickness of the PMZ eventually decreases again as crustal thickness exceeds 40–60 km (depending on which baseline recharge rate is adopted) because the basal magmatic flux becomes too low to support a thick PMZ. At crustal thicknesses of 50–60 km, 6–9 km of melt are available to be expelled to the upper crust in the form of plutons for baseline recharge rates of 10–15 $km^2 Myr^{-1}$. Only small amounts (<2 km) of melt are available for baseline recharge rates <10 $km^2 Myr^{-1}$.

Our results show that the thickness of the PMZ and its average temperature correlate for crustal thicknesses less than 30 km, but decouple at greater crustal thicknesses (Figure 6A). The hottest PMZs and hence most mafic interstitial melts are favored at intermediate

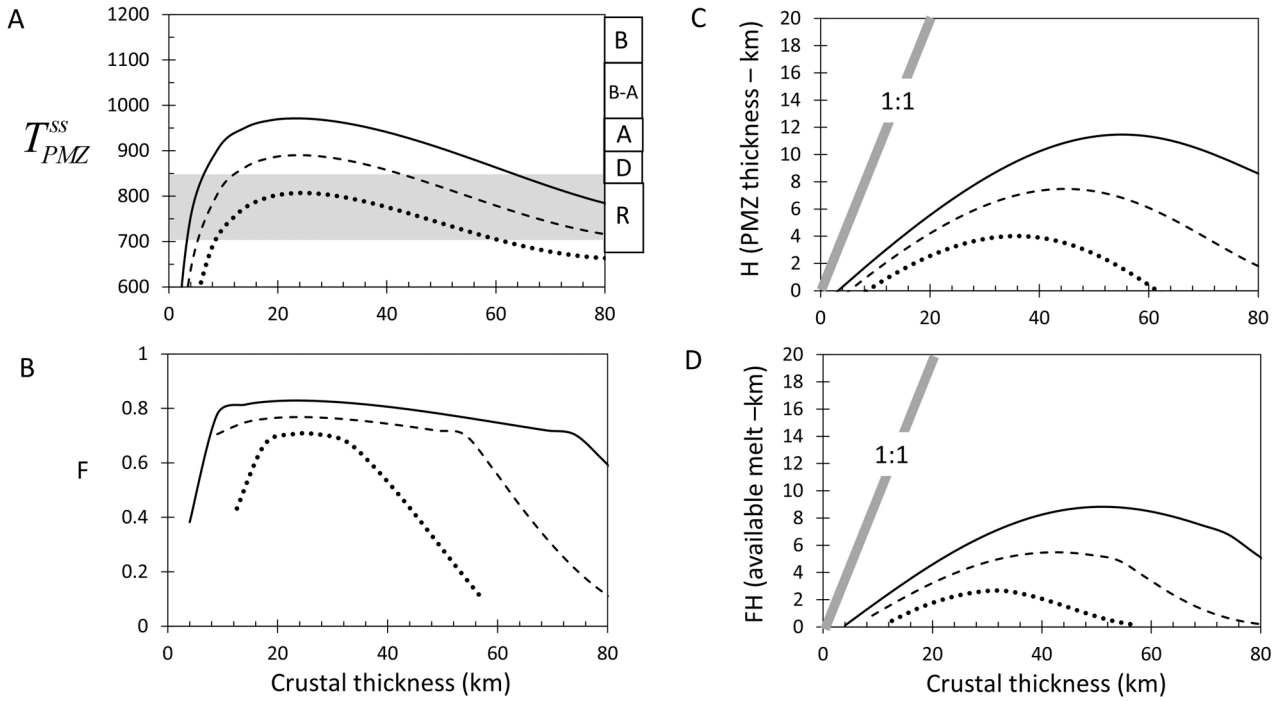

Figure 5: Characteristics of the lower crustal partially molten zone (PMZ) at steady state for a hydrous system. [A] Average steady state temperature of the PMZ (T^{SS}_{PMZ}) versus crustal thickness (km). Three curves are shown corresponding to different baseline levels of magmatic recharge rates J^o_{in} (km^2 Myr^{-1}) as shown in Figure 4. The inset shows how J_{in} decays with crustal thickness; a characteristic decay length of 20 km was assumed for all three cases. Solidus for a hydrous system is 700 °C. Gray zone represents temperature range of silicic plutons as inferred from Zr saturation temperatures [Miller et al. 1988; Lee 2014]. Right hand side bar represents approximate classification of magma type from Figure 4D. [B] Melt fraction (F) in the PMZ versus crustal thickness for different baseline levels of J^o_{in} as shown in A. A hydrous system was assumed. [C] Thickness (H) of the PMZ versus crustal thickness. Gray line represents 1:1 line where PMZ thickness equals crustal thickness. PMZ thickness never exceeds 20 % of the total crustal thickness. [D] Total available melt that can be extracted from the PMZ to the surface versus crustal thickness. This is determined by the product of F and H. All models are for a basal heat flow q_o of 15 mW m^{-2}.

crustal thicknesses (~20–25 km), but the total available volume of these mafic melts (FH), is low (<3 km). At crustal thicknesses of 40–80 km, typical of mature arcs, thick and intermediate temperature PMZs develop, and because of the great thickness of these PMZs, the total available volume of intermediate temperature interstitial melts, corresponding to andesitic and dacitic magmas, is large. Our calculations show for crustal thicknesses greater than 40 km, 6–9 km of intermediate magmas are available for transport to the upper crust in the form of voluminous plutons. If total available melt limits maximum pluton size, our model results are consistent with observations that the largest plutons tend to be andesitic or dacitic and favored when continental arc crust is thick.

In dry systems (Figure 6B), the general trends described above persist, but the predicted melt fractions and PMZ thicknesses contract substantially due to a higher solidus. (Figure 6B) shows the case in which the dry solidus is 200 °C higher than the wet solidus. These melts will be hot and mafic, but only small volumes are available. If magmas traversing thin crust are drier, as has been suggested [Lee 2014], the size and compositional differences of plutons traversing thin and thick crust would be accentuated, similar to what is seen in our study area (Figure 1). A pre-requisite for developing a thick PMZ is thus a hydrous system that drives depression of the solidus and widening of the PMZ. Superimposed on this effect is the effect of crustal thickness.

Finally, we note that at crustal thickness less than 20 km (Figure 6), our model predicts very cold PMZs and hence highly silicic interstitial liquids within the PMZ, in seeming contradiction to global observations that the silica content of arc magmas decreases with decreasing crustal thickness [Farner and Lee 2017]. However, for thin crust, predicted melt fractions F are so low that these cold melts might not always segregate. Instead, these cold PMZs in very thin crust may represent mafic magmas that have quickly frozen in place without allowing late-stage cold interstitial melts to escape, thereby preserving a mafic bulk composition.

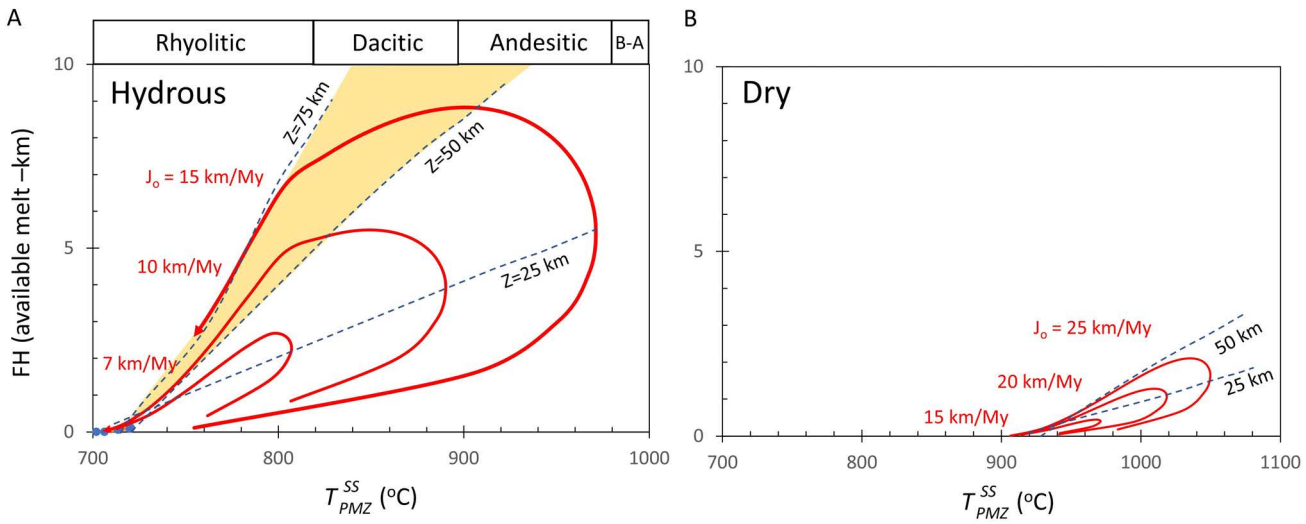

Figure 6: Total available melt (FH) that can be extracted from the PMZ and emplaced into the upper crust versus steady state temperature T^{SS}_{PMZ} of the PMZ. Top horizontal axis represents approximate composition of melt. Three scenarios are shown (red curves) for different baseline levels of magmatic recharge J^o_{in} . Arrow shows the direction of increasing crustal thickness. [A] is for a hydrous system with a wet solidus of 700 °C and liquidus of 1200 °C. [B] is for a dry system with a solidus of 900 °C and a 1200 °C liquidus. Dashed lines represent contours of crustal thickness. Basal heat flow of 15 mW m^{-2} assumed for [A] and [B].

Any differentiated melts that do escape would likely be of low F and cold, and thus, one would expect a bimodal terrane composed of both gabbros and highly silicic magmas, as seen in our study area and in global systematics of arc magmas [Farner and Lee 2017].

We can directly compare our model results to observed pluton area-SiO_2 relationships in (Figure 2D). While there does not appear to be any significant correlation between SiO_2 and pluton area because small plutons exist for all compositions, ranging from granites to gabbros, the largest plutons appear to be andesitic or dacitic in composition and hence are relatively cold. It is the maximum envelope of pluton sizes that is most relevant. There are few limitations to forming small plutons, but availability of melt, as modeled here, is a natural limit on the maximum size of plutons. Thus, if we examine the maximum pluton areas for a given SiO_2 content, we find maximum pluton size is small for mafic magmas, reaches a peak for andesitic/dacitic compositions, and declines again for rhyolitic compositions. This general behavior of maximum pluton size is consistent with our model results in Figure 6. We note, of course, that mapped pluton area does not necessarily scale with size because the pre-erosional vertical dimension is not known. However, the range of pluton areas from <10 km^2 to ~500 km^2 would require nearly a 50-fold difference between the original thicknesses of the smallest and largest plutons for these extremes to be of comparable volume, which is unreasonable. Thus, the differences in pluton area from the smallest to the largest are likely representative of differences in pluton size.

In summary, in thin crusts, cooling rates are high so the thickness of the lower crustal PMZ is small and the available amount of melt to make plutons of any composition is small. Cooling rates are so high that mafic magmas freeze in place and the only differentiated liquids are represented by very cold (750 °C) and highly silicic compositions, resulting in a bimodal distribution of pluton composition. As the crust thickens, cooling rates decline and the thickness of the lower crustal PMZ expands, increasing the availability of melts. These lower crustal PMZs in thick crust will be of intermediate temperatures (800–900 °C) and thus generate andesitic to dacitic magmas. Finally, in extremely thick crusts (>70 km), the thickness of the lower crustal PMZ contracts because, although cooling rates are slow, magmatic influx from the mantle is suppressed, reducing the advective addition of heat into the lower crust.

5 Conclusions and future work

In summary, we propose that the lower crust of active magmatic arcs is represented by long-lived PMZs sustained by inefficient heat loss through thick crust and by recharge of hydrous basaltic magmas. These PMZs are the source regions for the upper and mid-crustal plutons that form the backbones of continental arcs [Annen et al. 2005]. Our study explains the seemingly paradoxical observation that "cool" magmas generate large plutons [Bachmann and Bergantz 2008; Blatter et al. 2017]. Large and relatively cool PMZs are favored in thick arcs, explaining why andesitic/dacitic magmatism is so prevalent in mature continental arcs, but not in thin island arcs [Farner and Lee 2017]. Derivation

of the melts that feed plutons from a common long-lived lower crustal PMZ can also explain the remarkable compositional homogeneity of individual plutons and the apparent cogenetic compositions of plutons that are otherwise separated in time and space.

Cumulative recharge needed to sustain these PMZs will also enhance the concentrations of incompatible elements or components, such as chalcophile elements, water and CO_2, in the residual melts and may bear on why many porphyry ore deposits are found in thick and mature continental arcs [Chiaradia 2013; Lee 2014; Lee and Tang 2020; Park et al. 2021]. Our model also predicts significant recycling of mafic cumulates to the mantle, but while there is ample evidence for such recycling [Ducea and Saleeby 1998; Lee 2014; Jagoutz and Kelemen 2015], our study suggests that the removal of cumulates may be more continuous than the more discrete delamination scenarios often proposed. Finally, if the composition and magnitude of the magmatic flux in continental arcs is indeed controlled by crustal thickness, profound implications follow because crustal thickness in active arcs is the product of a complex interplay between magmatism, tectonic forcing and erosion [Lee et al. 2015b; Cao et al. 2020]. How the balance of these different processes varies in space and deep time may thus control the nature of continental crust formation throughout Earth's history [Clift 2004].

While there are many speculative parts and simplifications in this contribution, we believe that the observations and concepts presented here provide a fertile basis for future research. The next logical steps are to 1) model the PMZ under transient instead of steady state conditions and 2) explore the influence of erosion and hydrothermal circulation. Here, we also focused primarily on a fractionation origin of andesites and dacites, albeit with mixing implicit since we treat our PMZ as homogeneous. However, the effects of crustal assimilation and/or re-melting of the crust in our modeling framework and in generating felsic magmas should be explored in future studies. Our models also do not address the origin of andesites and dacites from direct melting of the mantle, but it seems unlikely that such an origin can explain the correlation between voluminous andesitic magmatism and crustal thickness. In any case, examining the spatial distribution, sizes and compositions of plutons in other arcs would go far in testing the concepts presented here.

Acknowledgements

This work was supported by the US NSF EAR – 1850832 and a Guggenheim Fellowship to Lee. We thank Douglas M. Morton for his inspiration and support. Discussions with Sydney Allen, Jackson Borchardt, Chen Chen, Patrick Phelps, Chenguang Sun, and Ming Tang are appreciated. We thank Wendy Bohrson and Peter Clift for detailed and useful reviews and Lynne Elkins for editorial handling.

Author contributions

Cin-Ty Lee developed the idea, compiled and synthesized the data, and wrote the manuscript. Both authors developed the model.

Data availability

All data are provided as Supplemental Materials.

Copyright notice

References

Almeev, R. R., T. Bolte, B. P. Nash, F. Holtz, M. Erdmann, and H. E. Cathey (2012). "High-temperature, low-H2O Silicic Magmas of the Yellowstone Hotspot: an Experimental Study of Rhyolite from the Bruneau–Jarbidge Eruptive Center, Central Snake River Plain, USA". *Journal of Petrology* 53.9, pp. 1837–1866. DOI: 10.1093/petrology/egs035.

Annen, C., J. D. Blundy, and R. S. J. Sparks (2005). "The Genesis of Intermediate and Silicic Magmas in Deep Crustal Hot Zones". *Journal of Petrology* 47.3, pp. 505–539. DOI: 10.1093/petrology/egi084.

Bachmann, O. and G. W. Bergantz (2008). "Rhyolites and their Source Mushes across Tectonic Settings". *Journal of Petrology* 49.12, pp. 2277–2285. DOI: 10.1093/petrology/egn068.

Baird, A., K. Baird, E. Welday, P. Abbott, and V. Todd (1979). "Batholithic rocks of the northern Peninsular and Transverse Ranges, southern California: Chemical composition and variation". *Mesozoic Crystalline Rocks: Peninsular Range Batholith and Pegmatites, Point Sal Ophiolite: San Diego, Department of Geological Sciences, San Diego State University*, pp. 111–132.

Barboni, M., C. Annen, and B. Schoene (2015). "Evaluating the construction and evolution of upper crustal magma reservoirs with coupled U/Pb zircon geochronology and thermal modeling: A case study from the Mt. Capanne pluton (Elba, Italy)". *Earth and Planetary Science Letters* 432, pp. 436–448. DOI: 10.1016/j.epsl.2015.09.043.

Blatter, D. L., T. W. Sisson, and W. B. Hankins (2017). "Voluminous arc dacites as amphibole reaction-boundary liquids". *Contributions to Mineralogy and Petrology* 172.5. doi: 10.1007/s00410-017-1340-6.

Bohrson, W. A., F. J. Spera, M. S. Ghiorso, G. A. Brown, J. B. Creamer, and A. Mayfield (2014). "Thermodynamic Model for Energy-Constrained Open-System Evolution of Crustal Magma Bodies Undergoing Simultaneous Recharge, Assimilation and Crystallization: the Magma Chamber Simulator". *Journal of Petrology* 55.9, pp. 1685–1717. doi: 10.1093/petrology/egu036.

Bohrson, W. A. and F. J. Spera (2007). "Energy-Constrained Recharge, Assimilation, and Fractional Crystallization (EC-RAχFC): A Visual Basic computer code for calculating trace element and isotope variations of open-system magmatic systems". *Geochemistry, Geophysics, Geosystems* 8.11.

Cao, W., C.-T. A. Lee, J. Yang, and A. V. Zuza (2019). "Hydrothermal circulation cools continental crust under exhumation". *Earth and Planetary Science Letters* 515, pp. 248–259. doi: 10.1016/j.epsl.2019.03.029.

Cao, W., J. Yang, A. V. Zuza, W.-Q. Ji, X.-X. Ma, X. Chu, and Q. P. Burgess (2020). "Crustal tilting and differential exhumation of Gangdese Batholith in southern Tibet revealed by bedrock pressures". *Earth and Planetary Science Letters* 543, p. 116347. doi: 10.1016/j.epsl.2020.116347.

Chiaradia, M. (2013). "Copper enrichment in arc magmas controlled by overriding plate thickness". *Nature Geoscience* 7.1, pp. 43–46. doi: 10.1038/ngeo2028.

Chin, E., C.-T. Lee, and J. Blichert-Toft (2015). "Growth of upper plate lithosphere controls tempo of arc magmatism: Constraints from Al-diffusion kinetics and coupled Lu-Hf and Sm-Nd chronology". *Geochemical Perspectives Letters* 1.1, pp. 20–32. doi: 10.7185/geochemlet.1503.

Clift, P. (2004). "Controls on tectonic accretion versus erosion in subduction zones: Implications for the origin and recycling of the continental crust". *Reviews of Geophysics* 42.2. doi: 10.1029/2003rg000127.

Collins, W. J., H.-Q. Huang, and X. Jiang (2016). "Water-fluxed crustal melting produces Cordilleran batholiths". *Geology* 44.2, pp. 143–146. doi: 10.1130/g37398.1.

Collins, W. J., J. B. Murphy, T. E. Johnson, and H.-Q. Huang (2020). "Critical role of water in the formation of continental crust". *Nature Geoscience* 13.5, pp. 331–338. doi: 10.1038/s41561-020-0573-6.

Draut, A. E., P. D. Clift, R. E. Hannigan, G. Layne, and N. Shimizu (2002). "A model for continental crust genesis by arc accretion: rare earth element evidence from the Irish Caledonides". *Earth and Planetary Science Letters* 203.3-4, pp. 861–877. doi: 10.1016/s0012-821x(02)00931-7.

Ducea, M. N., J. B. Saleeby, and G. Bergantz (2015). "The Architecture, Chemistry, and Evolution of Continental Magmatic Arcs". *Annual Review of Earth and Planetary Sciences* 43.1, pp. 299–331. doi: 10.1146/annurev-earth-060614-105049.

Ducea, M. and J. Saleeby (1998). "A Case for Delamination of the Deep Batholithic Crust beneath the Sierra Nevada, California". *International Geology Review* 40.1, pp. 78–93. doi: 10.1080/00206819809465199.

England, P. C. and R. F. Katz (2010). "Melting above the anhydrous solidus controls the location of volcanic arcs". *Nature* 467.7316, pp. 700–703. doi: 10.1038/nature09417.

Farner, M. J. and C.-T. A. Lee (2017). "Effects of crustal thickness on magmatic differentiation in subduction zone volcanism: A global study". *Earth and Planetary Science Letters* 470, pp. 96–107. doi: 10.1016/j.epsl.2017.04.025.

Grove, T. L., C. B. Till, and M. J. Krawczynski (2012). "The Role of H2O in Subduction Zone Magmatism". *Annual Review of Earth and Planetary Sciences* 40.1, pp. 413–439. doi: 10.1146/annurev-earth-042711-105310.

Hartung, E., G. Weber, and L. Caricchi (2019). "The role of H2O on the extraction of melt from crystallising magmas". *Earth and Planetary Science Letters* 508, pp. 85–96. doi: 10.1016/j.epsl.2018.12.010.

Hildreth, W. and S. Moorbath (1988). "Crustal contributions to arc magmatism in the Andes of Central Chile". *Contributions to Mineralogy and Petrology* 98.4, pp. 455–489. doi: 10.1007/bf00372365.

Jagoutz, O. and P. B. Kelemen (2015). "Role of Arc Processes in the Formation of Continental Crust". *Annual Review of Earth and Planetary Sciences* 43.1, pp. 363–404. doi: 10.1146/annurev-earth-040809-152345.

Jiang, H. and C.-T. A. Lee (2017). "Coupled magmatism-erosion in continental arcs: Reconstructing the history of the Cretaceous Peninsular Ranges batholith, southern California through detrital hornblende barometry in forearc sediments". *Earth and Planetary Science Letters* 472, pp. 69–81. doi: 10.1016/j.epsl.2017.05.009.

Karlstrom, L., C.-T. A. Lee, and M. Manga (2014). "The role of magmatically driven lithospheric thickening on arc front migration". *Geochemistry, Geophysics, Geosystems* 15.6, pp. 2655–2675. doi: 10.1002/2014gc005355.

Kelemen, P., K. Hanghoj, and A. Greene (2007). "One View of the Geochemistry of Subduction-Related Magmatic Arcs, with an Emphasis on Primitive Andesite and Lower Crust". *Treatise on Geochemistry*. Elsevier, pp. 1–70. doi: 10.1016/b0-08-043751-6/03035-8.

Kistler, R. W., J. L. Wooden, and D. M. Morton (2003). *Isotopes and ages in the northern Peninsular Ranges batholith, southern California*. US Department of the Interior, US Geological Survey.

Lara, M. and R. Dasgupta (2020). "Partial melting of a depleted peridotite metasomatized by a MORB-derived hydrous silicate melt - Implications for subduction zone magmatism". *Geochimica et Cosmochimica Acta* 290, pp. 137–161. DOI: 10.1016/j.gca.2020.09.001.

Lee, C.-T. (2014). "Physics and Chemistry of Deep Continental Crust Recycling". *Treatise on Geochemistry*. Elsevier, pp. 423–456. DOI: 10.1016/b978-0-08-095975-7.00314-4.

Lee, C.-T. A. and O. Bachmann (2014). "How important is the role of crystal fractionation in making intermediate magmas? Insights from Zr and P systematics". *Earth and Planetary Science Letters* 393, pp. 266–274. DOI: 10.1016/j.epsl.2014.02.044.

Lee, C.-T. A., D. M. Morton, M. J. Farner, and P. Moitra (2015a). "Field and model constraints on silicic melt segregation by compaction/hindered settling: The role of water and its effect on latent heat release". *American Mineralogist* 100.8-9, pp. 1762–1777. DOI: 10.2138/am-2015-5121.

Lee, C.-T. A. and M. Tang (2020). "How to make porphyry copper deposits". *Earth and Planetary Science Letters* 529, p. 115868. DOI: 10.1016/j.epsl.2019.115868.

Lee, C.-T. A., S. Thurner, S. Paterson, and W. Cao (2015b). "The rise and fall of continental arcs: Interplays between magmatism, uplift, weathering, and climate". *Earth and Planetary Science Letters* 425, pp. 105–119. DOI: 10.1016/j.epsl.2015.05.045.

Lee, C.-T. A., D. M. Morton, R. W. Kistler, and A. K. Baird (2007). "Petrology and tectonics of Phanerozoic continent formation: From island arcs to accretion and continental arc magmatism". *Earth and Planetary Science Letters* 263.3-4, pp. 370–387. DOI: 10.1016/j.epsl.2007.09.025.

Liu, B. and C.-T. Lee (2020). "Large Silicic Eruptions, Episodic Recharge, and the Transcrustal Magmatic System". *Geochemistry, Geophysics, Geosystems* 21.9. DOI: 10.1029/2020gc009220.

Martin, H., R. Smithies, R. Rapp, J.-F. Moyen, and D. Champion (2005). "An overview of adakite, tonalite-trondhjemite-granodiorite (TTG), and sanukitoid: relationships and some implications for crustal evolution". *Lithos* 79.1-2, pp. 1–24. DOI: 10.1016/j.lithos.2004.04.048.

Miller, C. F., E. B. Watson, and T. M. Harrison (1988). "Perspectives on the source, segregation and transport of granitoid magmas". *Earth and Environmental Science Transactions of the Royal Society of Edinburgh* 79.2-3, pp. 135–156. DOI: 10.1017/s0263593300014176.

Morton, D., R. Kistler, F. Miller, V. Langenheim, W. Premo, J. Wooden, P. Cossette, and R. Jachens (2014a). "Lakeview Mountains pluton: A dynamically emplaced pluton, northern Peninsular Ranges batholith, southern California". *Peninsular Ranges Batholith, Baja California and Southern California: Geological Society of America Memoir* 211, pp. 395–420.

Morton, D., F. Miller, R. Kistler, W. Premo, C. Lee, V. Langenheim, J. Wooden, L. Snee, B. Clausen, and P. Cossette (2014b). "Framework and petrogenesis of the northern Peninsular Ranges batholith, southern California". *Peninsular Ranges Batholith, Baja California and Southern California: Geological Society of America Memoir* 211, pp. 61–143.

Morton, D. M., F. K. Miller, P. M. Cossette, and K. R. Bovard (2006). *Geologic Map of the San Bernardino and Santa Ana 30' X 60' Quadrangles, California*. Citeseer.

Park, J.-W., I. H. Campbell, M. Chiaradia, H. Hao, and C.-T. Lee (2021). "Crustal magmatic controls on the formation of porphyry copper deposits". *Nature Reviews Earth & Environment*, pp. 1–16.

Rapp, R. P., N. Shimizu, and M. D. Norman (2003). "Growth of early continental crust by partial melting of eclogite". *Nature* 425.6958, pp. 605–609.

Reubi, O. and J. Blundy (2009). "A dearth of intermediate melts at subduction zone volcanoes and the petrogenesis of arc andesites". *Nature* 461.7268, pp. 1269–1273. DOI: 10.1038/nature08510.

Till, C. B., A. J. R. Kent, G. A. Abers, H. A. Janiszewski, J. B. Gaherty, and B. W. Pitcher (2019). "The causes of spatiotemporal variations in erupted fluxes and compositions along a volcanic arc". *Nature Communications* 10.1. DOI: 10.1038/s41467-019-09113-0.

Turner, S. J., C. H. Langmuir, R. F. Katz, M. A. Dungan, and S. Escrig (2016). "Parental arc magma compositions dominantly controlled by mantle-wedge thermal structure". *Nature Geoscience* 9.10, pp. 772–776. DOI: 10.1038/ngeo2788.